Physics Letters A 378 (2014) 1809–1815

Contents lists available at ScienceDirect

Physics Letters A

www.elsevier.com/locate/pla

High order three part split symplectic integrators: Efficient techniques for the long time simulation of the disordered discrete nonlinear Schrödinger equation

Ch. Skokos [a,b], E. Gerlach [c], J.D. Bodyfelt [d,*], G. Papamikos [e], S. Eggl [f]

[a] Physics Department, Aristotle University of Thessaloniki, GR-54124 Thessaloniki, Greece
[b] Department of Mathematics and Applied Mathematics, University of Cape Town, Rondebosch 7701, South Africa
[c] Lohrmann Observatory, Technical University Dresden, D-01062 Dresden, Germany
[d] Centre for Theoretical Chemistry & Physics, The New Zealand Institute for Advanced Study, Massey University, Albany, Private Bag 102904, North Shore City, Auckland 0745, New Zealand
[e] School of Mathematics, Statistics and Actuarial Science, University of Kent, Canterbury, CT2 7NF, UK
[f] IMCCE, Observatoire de Paris, 77 Avenue Denfert-Rochereau, F-75014 Paris, France

ARTICLE INFO

Article history:
Received 3 July 2013
Received in revised form 23 April 2014
Accepted 27 April 2014
Available online 1 May 2014
Communicated by R. Wu

Keywords:
Symplectic integrators
Three part split
Disorder
Nonlinear Schrödinger equation
Multidimensional Hamiltonian systems

ABSTRACT

While symplectic integration methods based on operator splitting are well established in many branches of science, high order methods for Hamiltonian systems that split in more than two parts have not been studied in great detail. Here, we present several high order symplectic integrators for Hamiltonian systems that can be split in exactly three integrable parts. We apply these techniques, as a practical case, for the integration of the disordered, discrete nonlinear Schrödinger equation (DDNLS) and compare their efficiencies. Three part split algorithms provide effective means to numerically study the asymptotic behavior of wave packet spreading in the DDNLS – a hotly debated subject in current scientific literature.

1. Introduction

Following the time evolution of a dynamical system is generally accomplished by solving its corresponding equations of motion. If, for instance, the system under consideration can be described by an autonomous Hamiltonian function $H(\vec{q},\vec{p})$, with $\vec{q}$, $\vec{p}$ respectively being vectors of the generalized coordinates and momenta, the equations of motion can be readily derived via Hamilton's equations. One then attempts to determine the solution $\vec{x}(t)=(\vec{q}(t),\vec{p}(t))$, $t>0$, for any given initial condition $\vec{x}(0)$. Formally this solution can be described by the action of the operator e^{tL_H}, with $L_H=\sum_i H_{p_i}\partial_{q_i}-H_{q_i}\partial_{p_i}$, on the initial condition, i.e. $\vec{x}(t)=e^{tL_H}\vec{x}(0)$. The Hamiltonian is said to be integrable if the action of this operator is known explicitly and the solution of the Hamilton equations of motion can be written in a closed, analytic form. Unfortunately, this task is rarely possible, but in most cases the true solution can be approximated numerically. General purpose numerical integration methods for ordinary differential equations are capable of providing such approximations.

In this respect, the so-called symplectic integration techniques are of particular interest, as they are explicitly designed for the integration of Hamiltonian systems (see, for example, Chap. VI of [1–3] and references therein). Assume that $H(\vec{q},\vec{p})$ can be written as $H(\vec{q},\vec{p})=A(\vec{q},\vec{p})+B(\vec{q},\vec{p})$, so that the action of operators e^{tL_A} and e^{tL_B} is known, and the solution of their Hamilton equations of motion can be written analytically, while $e^{\tau L_H}$ does not permit a closed analytical solution of its equations of motion. Then, a symplectic scheme for integrating the equations of motion from time t to time $t+\tau$ consists of approximating the operator $e^{\tau L_H}=e^{\tau(L_A+L_B)}$ by a product of j operators $e^{c_i\tau L_A}$ and $e^{d_i\tau L_B}$, which represent exact integrations of Hamiltonians $A(\vec{q},\vec{p})$ and $B(\vec{q},\vec{p})$ over times $c_i\tau$ and $d_i\tau$ respectively, i.e. $e^{\tau L_H}=\prod_{i=1}^{j}e^{c_i\tau L_A}e^{d_i\tau L_B}+\mathcal{O}(\tau^{n+1})$. The constants c_i and d_i are appropriately chosen to increase the order of the remainder of this approximation. In practice, using this symplectic integrator (SI) we approximate the dynamics of the real Hamiltonian $H=A+B$ by a new one, $K=A+B+\mathcal{O}(\tau^n)$, introducing an error term of order τ^n in each integration step – the SI is then said to be of order n.

* Corresponding author.
E-mail addresses: haris.skokos@uct.ac.za (Ch. Skokos), J.Bodyfelt@massey.ac.nz (J.D. Bodyfelt).

http://dx.doi.org/10.1016/j.physleta.2014.04.050
0375-9601/

By their construction SIs preserve the symplectic nature of the Hamiltonian system and keep bounded the error of the computed value of H (which is an integral of the system, commonly referred as the 'energy') irrespectively of the total integration time. Generally, this is not the case with non-symplectic integration algorithms. Furthermore, many SIs permit the use of relatively large integration time steps τ for acceptable levels of energy accuracy, resulting in lower CPU time requirements. Due to these benefits, SIs became a standard technique in Hamiltonian dynamics with particular importance in long time integrations of multidimensional systems. Several SIs of different orders based on this operator splitting have been developed over the years by various researchers [4–13].

2. Three part split symplectic integrators

In many cases the Hamiltonian can be written as a sum of the system's kinetic energy $T(\vec{p})$, dependent only on the momenta $\vec{p}$, and the potential $V(\vec{q})$, dependent only on the positions $\vec{q}$. Then the obvious choice for the application of a SI is to consider $A \equiv T(\vec{p})$ and $B \equiv V(\vec{q})$. Yet in many physical problems, the corresponding Hamiltonian cannot be split in two integrable parts – is it possible to exploit the advantages of SIs for such systems as well? The answer to this question is positive as, theoretically, symplectic integration schemes can be constructed for Hamiltonian systems that split in an arbitrary number of integrable parts [14], [1, Sect. II.5]. Of course, the construction of high order SIs is not an easy task as the number of involved operators increase extremely fast. This problem becomes even more complicated when the Hamiltonian is split in three, instead of two, integrable parts.

In this paper we systematically present and test the performance of efficient high order SIs for Hamiltonians that can be split in three integrable parts. Particular cases of second order three part split SIs, connected with astronomical problems, have been reported in literature [15–18]. In these works, the considered Hamiltonians were expressed as $H = A(\vec{q},\vec{p}) + B(\vec{q},\vec{p}) + C(\vec{q},\vec{p})$, the action of operators $e^{\tau L_A}$, $e^{\tau L_B}$ and $e^{\tau L_C}$ was analytically obtained, the second order SI of 5 steps

$$\mathrm{ABC}^2(\tau) = e^{\frac{\tau}{2}L_A} e^{\frac{\tau}{2}L_B} e^{\tau L_C} e^{\frac{\tau}{2}L_B} e^{\frac{\tau}{2}L_A} \tag{1}$$

was constructed, and its performance was studied. This integrator represents the simplest form of a symmetric SI that can be constructed for a Hamiltonian which splits in three distinct parts, as was also explained in [19].

Some attempts to create three part split SIs of order higher than two can be found in the literature. In [19] an integrator of order four was obtained, while in [20] second and fourth order integration schemes for a particular complicated molecular model were presented. Recently, in [12,13] three part split SIs especially oriented for near integrable Hamiltonians of the form $H = A + \epsilon(B + C)$, with $\epsilon \ll 1$, were constructed and applied to a specific astronomical problem. In principle these integrators can be applied to any Hamiltonian that split in three integrable parts, and we will use some of them later on in Section 3.1.

A general way to obtain higher order SIs is the construction of symmetric compositions of a basic symmetric second order integrator. The number of times that this basic integrator is used in a particular scheme determines the number of '*stages*' of the constructed integrator. This approach led to the creation of efficient schemes of order six, eight and ten [21,22] (see also [23] for a detailed review of these methods), but to the best of our knowledge, it has never been systematically applied to Hamiltonians that split in three integrable parts.

2.1. Integrators of order four

We start the presentation of three part split methods by implementing an algorithm based on the composition technique proposed by Yoshida [4]. Starting from a SI $S^{2n}(\tau)$ of order $2n$, we can construct a SI $S^{2n+2}(\tau)$ of order $2n+2$, as

$$S^{2n+2}(\tau) = S^{2n}(z_1\tau) S^{2n}(z_0\tau) S^{2n}(z_1\tau), \tag{2}$$

with $z_0 = -2^{1/(2n+1)}/[2 - 2^{1/(2n+1)}]$ and $z_1 = 1/[2 - 2^{1/(2n+1)}]$. Applying this procedure to the second order SI (1) we obtain the fourth order SI of 3 stages and 13 steps

$$\mathrm{ABC}^4_{[\mathrm{Y}]}(\tau) = \mathrm{ABC}^2(x_1\tau)\mathrm{ABC}^2(x_0\tau)\mathrm{ABC}^2(x_1\tau), \tag{3}$$

with

$$x_0 = \frac{-\sqrt[3]{2}}{2-\sqrt[3]{2}}, \qquad x_1 = \frac{1}{2-\sqrt[3]{2}}, \tag{4}$$

and the subscript [Y] referring to the author of [4]. We note that the $\mathrm{ABC}^4_{[\mathrm{Y}]}$ was explicitly constructed in [19].

We also consider another composition scheme which was introduced in [24] and studied in [21] (where it was named 's5odr4') and [22]. This scheme has 5 stages and starting from a second order SI, which in our case will be the ABC^2 integrator (1), leads to the fourth order integrator

$$\begin{aligned}\mathrm{ABC}^4_{[\mathrm{S}]}(\tau) = {} & \mathrm{ABC}^2(p_2\tau)\mathrm{ABC}^2(p_2\tau)\mathrm{ABC}^2\big((1-4p_2)\tau\big) \\ & \times \mathrm{ABC}^2(p_2\tau)\mathrm{ABC}^2(p_2\tau),\end{aligned} \tag{5}$$

with

$$p_2 = \frac{1}{4-\sqrt[3]{4}}, \qquad 1 - 4p_2 = -\frac{\sqrt[3]{4}}{4-\sqrt[3]{4}}, \tag{6}$$

which has 21 steps. As in the previous case the subscript [S] refers to the author of [24].

2.2. Integrators of order six

Eq. (2) can be used repeatedly to get higher order three part split SIs. Although such a procedure for obtaining arbitrary SIs of even order with exact coefficients is straightforward, it is not optimal with respect to the number of required steps. As was already pointed out in [4], alternative methods can be applied to obtain more economical integrators of high order, although the new coefficients can no longer be given in analytical form. Several sixth order SIs of this kind were presented in [4]. Here, we consider one corresponding to 'solution A' in [4]

$$\begin{aligned}\mathrm{ABC}^6_{[\mathrm{Y}]}(\tau) = {} & \mathrm{ABC}^2(w_3\tau)\mathrm{ABC}^2(w_2\tau)\mathrm{ABC}^2(w_1\tau)\mathrm{ABC}^2(w_0\tau) \\ & \times \mathrm{ABC}^2(w_1\tau)\mathrm{ABC}^2(w_2\tau)\mathrm{ABC}^2(w_3\tau)\end{aligned} \tag{7}$$

having 7 stages and 29 steps. The exact values of w_i, $i = 0, 1, 2, 3$, can be found in [1, Chap. V, Eq. (3.11)] and [4]. We include this particular integrator in our study because according to [25] it shows the best behavior among the ones presented in [4]. We also note that this integrator corresponds to the 's7odr6' method studied in [21].

In addition we include in our study other SIs of order six obtained by composition techniques which involve more stages than the $\mathrm{ABC}^6_{[\mathrm{Y}]}$ integrator. In particular we consider the 's9odr6b' integrator of [21] which has 9 stages, i.e. 9 implementations of a second order SI. Using the ABC^2 method (1) as such an integrator we end up with the scheme

$$\mathrm{ABC}^6_{[\mathrm{KL}]}(\tau) = \mathrm{ABC}^2(\delta_1\tau)\mathrm{ABC}^2(\delta_2\tau)\mathrm{ABC}^2(\delta_3\tau)\mathrm{ABC}^2(\delta_4\tau)\mathrm{ABC}^2(\delta_5\tau) \times \mathrm{ABC}^2(\delta_4\tau)\mathrm{ABC}^2(\delta_3\tau)\mathrm{ABC}^2(\delta_2\tau)\mathrm{ABC}^2(\delta_1\tau) \quad (8)$$

of 37 steps. We note that the subscript [KL] refers to the initials of the authors of [21], and the exact values of constants δ_i, $1 \leqslant i \leqslant 5$, are given in the appendix of [21].

We also consider a sixth order SI based on a composition method with 11 stages, which was introduced in [22]. This approach leads to the SI

$$\mathrm{ABC}^6_{[\mathrm{SS}]}(\tau) = \mathrm{ABC}^2(\gamma_1\tau)\mathrm{ABC}^2(\gamma_2\tau)\cdots\mathrm{ABC}^2(\gamma_5\tau)\mathrm{ABC}^2(\gamma_6\tau) \times \mathrm{ABC}^2(\gamma_5\tau)\cdots\mathrm{ABC}^2(\gamma_2\tau)\mathrm{ABC}^2(\gamma_1\tau) \quad (9)$$

which has 45 individual steps. Again the subscript [SS] refers to the authors of [22], while the exact values of γ_i, $1 \leqslant i \leqslant 6$, are given in Eq. (11) of [22].

2.3. Integrators of order eight

In [4] five different composition methods of 15 stages that lead to eighth order SIs are given. Among them the one named 'solution D' exhibits the best behavior according to [22,25]. For this reason we include this composition method in our study. The resulting SI (using the constants w_i, $0 \leqslant i \leqslant 7$, appearing in Table 2 of [4]) is

$$\mathrm{ABC}^8_{[\mathrm{Y}]}(\tau) = \mathrm{ABC}^2(w_7\tau)\mathrm{ABC}^2(w_6\tau)\cdots\mathrm{ABC}^2(w_1\tau)\mathrm{ABC}^2(w_0\tau) \times \mathrm{ABC}^2(w_1\tau)\cdots\mathrm{ABC}^2(w_6\tau)\mathrm{ABC}^2(w_7\tau) \quad (10)$$

having 61 individual steps.

We also consider two more SIs of order eight obtained by composition techniques which involve more stages than the $\mathrm{ABC}^8_{[\mathrm{Y}]}$ integrator. The first is based on the 's17odr8b' integrator of [21] which has 17 stages. Its form is

$$\mathrm{ABC}^8_{[\mathrm{KL}]}(\tau) = \mathrm{ABC}^2(\delta_1\tau)\mathrm{ABC}^2(\delta_2\tau)\cdots\mathrm{ABC}^2(\delta_8\tau)\mathrm{ABC}^2(\delta_9\tau) \times \mathrm{ABC}^2(\delta_8\tau)\cdots\mathrm{ABC}^2(\delta_2\tau)\mathrm{ABC}^2(\delta_1\tau). \quad (11)$$

This integrator has 69 steps and its coefficients can be found in the appendix of [21]. The second integrator is

$$\mathrm{ABC}^8_{[\mathrm{SS}]}(\tau) = \mathrm{ABC}^2(\gamma_1\tau)\mathrm{ABC}^2(\gamma_2\tau)\cdots\mathrm{ABC}^2(\gamma_9\tau)\mathrm{ABC}^2(\gamma_{10}\tau) \times \mathrm{ABC}^2(\gamma_9\tau)\cdots\mathrm{ABC}^2(\gamma_2\tau)\mathrm{ABC}^2(\gamma_1\tau) \quad (12)$$

and is based on a composition method with 19 stages presented in Eq. (13) of [22].

2.4. An integrator of order ten

Finally, as an extreme case, we include in our study a SI of order ten. In particular we consider the tenth order composition method of 31 stages presented in Eq. (15) of [22], which leads to the SI

$$\mathrm{ABC}^{10}_{[\mathrm{SS}]}(\tau) = \mathrm{ABC}^2(\gamma_1\tau)\mathrm{ABC}^2(\gamma_2\tau)\cdots\mathrm{ABC}^2(\gamma_{15}\tau)\mathrm{ABC}^2(\gamma_{16}\tau) \times \mathrm{ABC}^2(\gamma_{15}\tau)\cdots\mathrm{ABC}^2(\gamma_2\tau)\mathrm{ABC}^2(\gamma_1\tau) \quad (13)$$

with 125 steps. We choose to not include additional integrators of order ten based on composition techniques with more stages due to the substantial increase of their complexity.

In Table 1 we present all the three part split SIs used in our study providing information about their order, the number of their stages and steps, as well as references for obtaining the values of their coefficients.

Table 1
Information for the three part split SIs of Section 2. For each integrator we provide its name, its order, the number of its stages (i.e. the appearances of the second order SI ABC^2 (1)) and the total number of individual steps. In the last column (named 'Coefficients') we indicate where the explicit values of the coefficients appearing in each step can be found. For example (4) refers to Eq. (4) of this paper.

SI	Order	Stages	Steps	Coefficients
ABC^2	2	1	5	(1)
$\mathrm{ABC}^4_{[\mathrm{Y}]}$	4	3	13	(4)
$\mathrm{ABC}^4_{[\mathrm{S}]}$	4	5	21	(6)
$\mathrm{ABC}^6_{[\mathrm{Y}]}$	6	7	29	'Solution A' in Table 1 of [4]
$\mathrm{ABC}^6_{[\mathrm{KL}]}$	6	9	37	Table 's9odr6b' in the appendix of [21]
$\mathrm{ABC}^6_{[\mathrm{SS}]}$	6	11	45	Equation (11) of [22]
$\mathrm{ABC}^8_{[\mathrm{Y}]}$	8	15	61	'Solution D' in Table 2 of [4]
$\mathrm{ABC}^8_{[\mathrm{KL}]}$	8	17	69	Table 's17odr8b' in the appendix of [21]
$\mathrm{ABC}^8_{[\mathrm{SS}]}$	8	19	77	Equation (13) of [22]
$\mathrm{ABC}^{10}_{[\mathrm{SS}]}$	10	31	125	Equation (15) of [22]

3. Integration of the disordered discrete nonlinear Schrödinger equation

In order to investigate the efficiency of the different SI schemes we choose a multidimensional Hamiltonian system describing a one-dimensional chain of coupled, nonlinear oscillators. In particular we consider the Hamiltonian of the disordered discrete nonlinear Schrödinger equation (DDNLS)

$$\mathcal{H}_D = \sum_l \epsilon_l|\psi_l|^2 + \frac{\beta}{2}|\psi_l|^4 - \left(\psi_{l+1}\psi_l^* + \psi_{l+1}^*\psi_l\right), \quad (14)$$

with complex variables ψ_l, lattice site indices l and nonlinearity strength $\beta \geqslant 0$. The random on–site energies ϵ_l are chosen uniformly from the interval $[-\frac{W}{2}, \frac{W}{2}]$, with W denoting the disorder strength. This model has two integrals of motion, as it conserves both the energy (14) and the norm $S = \sum_l |\psi_l|^2$, and has been extensively investigated in order to determine the characteristics of energy spreading in disordered systems [26–31]. These studies showed that the second moment, m_2, of the norm distribution grows subdiffusively in time t, as t^a, and the asymptotic value $a = 1/3$ of the exponent was theoretically predicted and numerically verified. Currently open questions on the dynamics of disordered systems concern the possible halt of wave packet's spreading for $t \to \infty$ [32,33], as well as the characteristics of its chaotic behavior. Thus, providing the means to perform accurate long time simulations for the DDNLS model within reasonable amounts of computational time is essential.

Applying the canonical transformation $\psi_l = (q_l + ip_l)/\sqrt{2}$, $\psi_l^* = (q_l - ip_l)/\sqrt{2}$, one can split (14) into a sum of three integrable parts A, B and C as follows

$$H_D = \sum_l \underbrace{\frac{\epsilon_l}{2}\left(q_l^2 + p_l^2\right) + \frac{\beta}{8}\left(q_l^2 + p_l^2\right)^2}_{A} \underbrace{-p_{l+1}p_l}_{B} \underbrace{-q_{l+1}q_l}_{C}, \quad (15)$$

where q_l and p_l are respectively generalized coordinates and momenta. For these three parts the propagation of initial conditions (q_l, p_l) at time t, to their final values (q_l', p_l') at time $t + \tau$ is given by the operators

$$e^{\tau L_A}: \begin{cases} q_l' = q_l\cos(\alpha_l\tau) + p_l\sin(\alpha_l\tau), \\ p_l' = p_l\cos(\alpha_l\tau) - q_l\sin(\alpha_l\tau), \end{cases} \quad (16)$$

$$e^{\tau L_B}: \begin{cases} p_l' = p_l, \\ q_l' = q_l - (p_{l-1} + p_{l+1})\tau, \end{cases} \quad (17)$$

$$e^{\tau L_C}: \begin{cases} q_l' = q_l, \\ p_l' = p_l + (q_{l-1} + q_{l+1}),\ \tau \end{cases} \quad (18)$$

with $\alpha_l = \epsilon_l + \beta(q_l^2 + p_l^2)/2$. Thus, the DDNLS model represents an ideal test case for our aforementioned three part split SIs.

3.1. Alternative integration approaches

In order to evaluate the efficiency of the integration schemes presented in Section 2, we compare their performance to that of other numerical techniques. In [27–30] numerical integration schemes based on traditional two part split SIs were applied for the integration of Hamiltonian (15). These approaches were based on the split of (15) in two parts as $\mathcal{A} = A$ and $\mathcal{B} = B + C$, and the application of second order SIs of the so-called SABA-family [11]; note that the $SABA_1$ integrator is more popularly known as the Störmer–Verlet leapfrog integrator.

In our study we implement the second order SI $SABA_2$ using the split $H_D = \mathcal{A} + \mathcal{B}$. The integration of the $\mathcal{A}$ part is performed according to (16), while different approaches for approximating the action of $e^{\tau L_{\mathcal{B}}} = e^{\tau L_{B+C}}$ are followed. In [27,28] a numerical scheme based on Fourier transforms was implemented (see appendix of [28] for more details) leading to a second order integrator with 5 steps, which we name $SIFT^2$ in the following. Another approach is to split the $\mathcal{B}$ part in two integrable parts as $\mathcal{B} = B + C$ and use the $SABA_2$ SI to approximate its solution. This means that we perform two successive two part splits in order to integrate H_D. This approach leads to a second order SI with 13 steps which we name SS^2 (this scheme corresponds to the PQ method used in [30]).

Extending the approach to split H_D (15) in two parts where the $\mathcal{A} = A$ is integrable and the $\mathcal{B} = B + C$ part is approximately integrated either by another two part split SI or by an appropriate Fourier transform scheme, we construct fourth order integrators, which, to the best of our knowledge, have never being used before for the integration of the DDNLS system. In particular, by applying the composition procedure (2) to the SS^2 integrator we construct a fourth order integrator with 37 simple steps that we call SS^4. Following a similar approach for the $SIFT^2$ integrator we obtain a fourth order integrator with 13 steps, which we name $SIFT^4$.

In addition, we use some recently introduced SIs [12,13] which were particularly constructed for nearly integrable Hamiltonians, i.e. Hamiltonians of the form $H = \mathcal{A} + \epsilon\mathcal{B}$, where the $\mathcal{A} = A$ part is integrable and $\epsilon \ll 1$. In particular, we consider the fourth order integrators ABA864, ABA1064, ABAH864, ABAH1064, where the $\mathcal{A}$ part is integrated explicitly and the $\mathcal{B}$ part either by the Fourier transforms (for the ABA864, ABA1064 integrators) or by the $SABA_2$ SI (for the ABAH864, ABAH1064 integrators). We note that the ABAH864 and ABAH1064 schemes were constructed from the ABA864 and ABA1064 integrators respectively, by assuming that the $\mathcal{B}$ part is a second order symmetric integrator [12] (which in our study is the $SABA_2$ scheme). This assumption leads to an additional condition of the integrator's coefficients, which in turn results to the addition of some more steps in the integrator. As the solution of the $\mathcal{B}$ part by Fourier transforms is a rather time consuming procedure, we decided to use this approach for solving the $\mathcal{B}$ part when applying the ABA864 and ABA1064 methods which have less individual steps.

In particular, based on the ABA864 and ABA1064 integrators of [12] we consider the fourth order schemes

$$\begin{aligned} SIFT^4_{864}(\tau) = {} & e^{\alpha_1 \tau L_A} e^{b_1 \tau L_{\mathcal{B}}} e^{\alpha_2 \tau L_A} e^{b_2 \tau L_{\mathcal{B}}} \cdots e^{\alpha_4 \tau L_A} e^{b_4 \tau L_{\mathcal{B}}} e^{\alpha_4 \tau L_A} \\ & \times e^{b_3 L_{\mathcal{B}}} e^{\alpha_3 \tau L_A} e^{b_2 \tau L_{\mathcal{B}}} e^{\alpha_2 \tau L_A} e^{b_1 \tau L_{\mathcal{B}}} e^{\alpha_1 \tau L_A} \end{aligned} \tag{19}$$

and

$$\begin{aligned} SIFT^4_{1064}(\tau) = {} & e^{\alpha_1 \tau L_A} e^{b_1 \tau L_{\mathcal{B}}} e^{\alpha_2 \tau L_A} e^{b_2 \tau L_{\mathcal{B}}} \cdots e^{\alpha_4 \tau L_A} e^{b_4 \tau L_{\mathcal{B}}} e^{\alpha_5 \tau L_A} \\ & \times e^{b_4 \tau L_{\mathcal{B}}} e^{\alpha_4 \tau L_A} \cdots e^{b_2 \tau L_{\mathcal{B}}} e^{\alpha_2 \tau L_A} e^{b_1 \tau L_{\mathcal{B}}} e^{\alpha_1 \tau L_A}, \end{aligned} \tag{20}$$

with 43 and 49 steps respectively, where the $\mathcal{B} = B + C$ part is integrated according to the Fourier transform procedure presented in [28]. The values of the coefficients appearing in (19) and (20) are given in Table 3 of [12].

Similarly, based on the ABAH864 and ABAH1064 integrators of [12] we consider the fourth order integrators

$$\begin{aligned} SS^4_{864}(\tau) = {} & e^{\alpha_1 \tau L_A} e^{b_1 \tau L_{\mathcal{B}}} e^{\alpha_2 \tau L_A} e^{b_2 \tau L_{\mathcal{B}}} \cdots e^{\alpha_4 \tau L_A} e^{b_4 \tau L_{\mathcal{B}}} e^{\alpha_5 \tau L_A} \\ & \times e^{b_4 \tau L_{\mathcal{B}}} e^{\alpha_4 \tau L_A} \cdots e^{b_2 \tau L_{\mathcal{B}}} e^{\alpha_2 \tau L_A} e^{b_1 \tau L_{\mathcal{B}}} e^{\alpha_1 \tau L_A} \end{aligned} \tag{21}$$

and

$$\begin{aligned} SS^4_{1064}(\tau) = {} & e^{\alpha_1 \tau L_A} e^{b_1 \tau L_{\mathcal{B}}} e^{\alpha_2 \tau L_A} e^{b_2 \tau L_{\mathcal{B}}} \cdots e^{\alpha_5 \tau L_A} e^{b_5 \tau L_{\mathcal{B}}} e^{\alpha_5 \tau L_A} \\ & \times e^{b_4 \tau L_{\mathcal{B}}} e^{\alpha_4 \tau L_A} \cdots e^{b_2 \tau L_{\mathcal{B}}} e^{\alpha_2 \tau L_A} e^{b_1 \tau L_{\mathcal{B}}} e^{\alpha_1 \tau L_A}, \end{aligned} \tag{22}$$

with 49 and 55 steps respectively, where the $\mathcal{B} = B + C$ part is integrated by the $SABA_2$ SI. The values of the coefficients appearing in (21) and (22) are given in Table 4 of [12].

Of course, one can also use any general purpose non-symplectic integrator for the integration of (15). One disadvantage of such techniques is that different epochs of the system's evolution are computed with different accuracy since these integrators do not keep the energy error bounded, but increase it as time increases. In particular for the DDNLS model considered here the later stages of its evolution, which are of most importance since we are mainly interested in the asymptotic behavior of the system, are computed less accurately. As a representative of non-symplectic integrators we consider here the variable step Runge–Kutta method called DOP853 [34], whose performance is controlled by the so-called one-step accuracy δ.

4. Numerical results

In order to compare the performance of the various integration schemes we consider a particular disorder realization of the DDNLS model (15) with $N = 1024$ lattice sites. We fix the total norm of the system to $S = 1$, and following [29] we initially excite homogeneously 21 central sites by attributing to each one of them the same constant norm, but with a random phase, while for all other sites we set $q_l(0) = p_l(0) = 0$. Due to the nonlinear nature of the model the norm distribution spreads, keeping of course the total norm $S = \sum_l (q_l^2 + p_l^2)/2$ constant ($S = 1$). The performance of the integration schemes is evaluated by their ability to (a) reproduce correctly the dynamics, which is reflected in the subdiffusive increase of $m_2(t)$, (b) keep the values of the two integrals H_D, S constant, as monitored by the evolution of the absolute relative errors of the energy $E_r(t) = |[H_D(t) - H_D(0)]/H_D(0)|$, and norm $S_r(t) = |[S(t) - S(0)]/S(0)|$, and (c) reduce the required CPU time $T_c(t)$ for the performed computations.

Results obtained by the second order SIs ABC^2, SS^2 and $SIFT^2$ and the non-symplectic integrator DOP853 are presented in Fig. 1. These integration methods correctly describe the system's dynamical evolution since for all of them the wave packet's m_2 shows practically the same behavior (Fig. 1a). The time steps τ of the three SIs were chosen so that all of them keep the relative energy error practically constant at $E_r \approx 10^{-5}$ (Fig. 1b). Since we are interested in the accurate long time integration of the DDNLS model we use $\delta = 10^{-16}$ for the implementation of the DOP853 integrator. For $t \approx 10^8$ (which can be considered as a typical final integration time for long time simulations), this choice results practically in the same energy error obtained by all other tested integrators. From Fig. 1c we see that the relative norm error S_r increases for all used methods, exhibiting larger values yet lower increase rates, for the ABC^2 and SS^2 SIs. Nevertheless, our results indicate that all methods can keep S_r to acceptable levels (e.g. $S_r \lesssim 10^{-2}$), even for long time integrations. It is worth noting that the Fourier transforms used by the $SIFT^2$ scheme for the integration of the $\mathcal{B}$ part

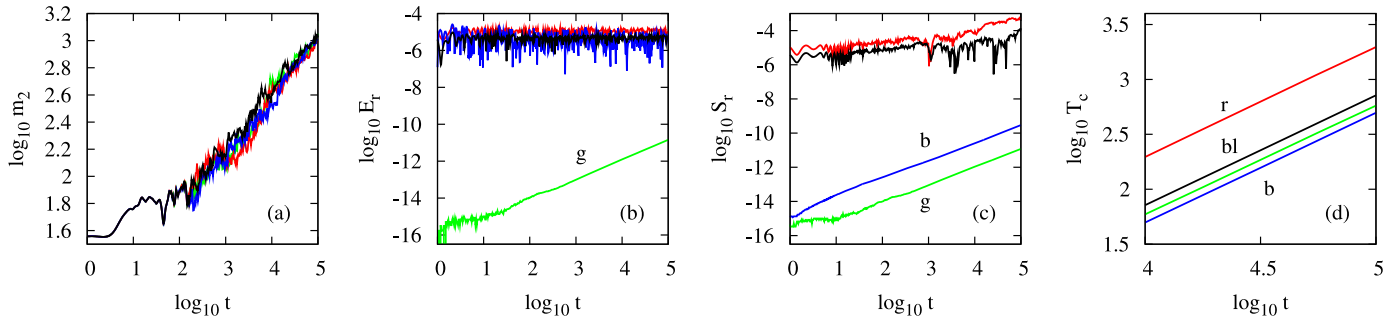

Fig. 1. (Color online.) Results for the integration of H_D (15) by the second order SIs ABC^2 for $\tau = 0.005$, SS^2 for $\tau = 0.02$, SIFT^2 for $\tau = 0.05$ [(r) red; (bl) black; (b) blue], and the non-symplectic integrator DOP853 for $\delta = 10^{-16}$ [(g) green]: time evolution of the logarithm of (a) the second moment $m_2(t)$, (b) the absolute relative energy error $E_r(t)$, (c) the absolute relative norm error $S_r(t)$, and (d) the required CPU time $T_c(t)$ in seconds.

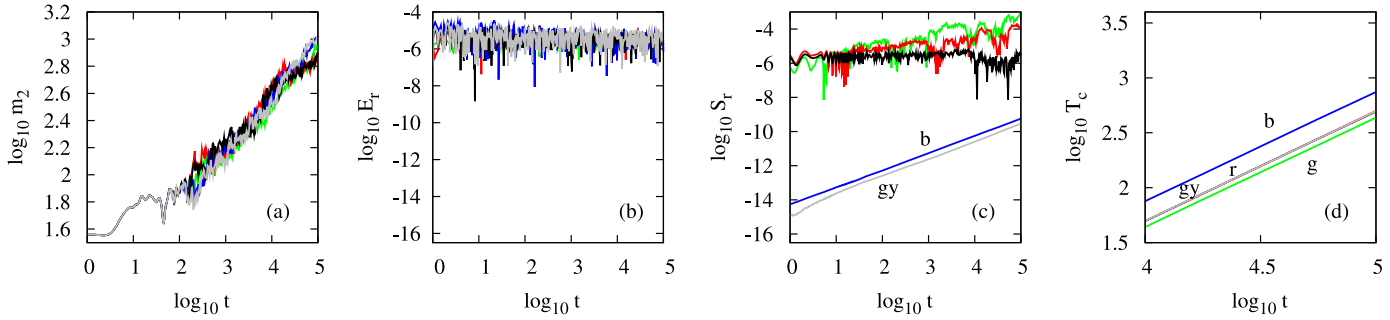

Fig. 2. (Color online.) Results for the integration of H_D (15) by the second order SI SIFT^2 for $\tau = 0.05$ [(gy) grey], and the fourth order SIs ABC$^4_{[Y]}$ for $\tau = 0.05$, ABC$^4_{[S]}$ for $\tau = 0.1$, SIFT^4 for $\tau = 0.125$ and SS^4 for $\tau = 0.1$ [(g) green; (r) red; (b) blue; (bl) black]. The panels are as in Fig. 1. Note that in panel (d) the red, grey, and black curves practically overlap.

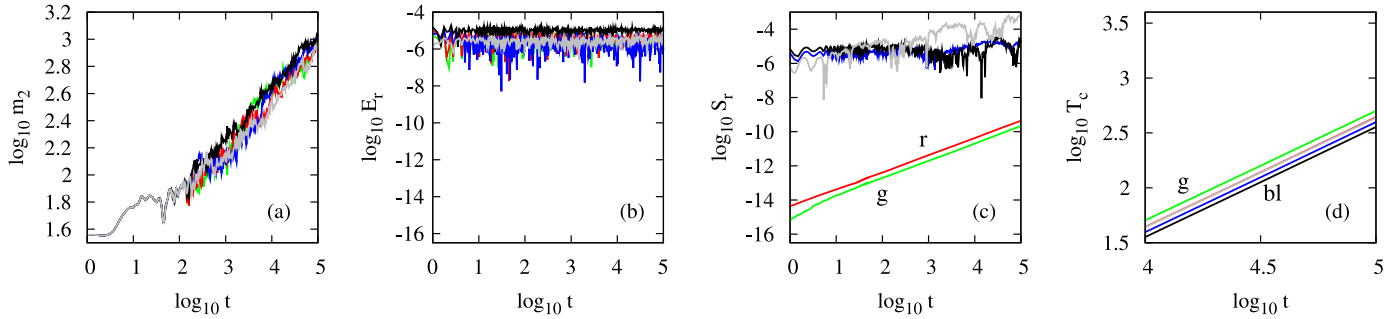

Fig. 3. (Color online.) Results for the integration of H_D (15) by the fourth order SI ABC$^4_{[Y]}$ for $\tau = 0.05$ [(gy) grey], and the fourth order SIs SIFT$^4_{864}$ for $\tau = 0.25$, SIFT$^4_{1064}$ for $\tau = 0.25$, SS$^4_{864}$ for $\tau = 0.25$ and SS$^4_{1064}$ for $\tau = 0.25$ [(r) red; (g) green; (bl) black; (b) blue]. The panels are as in Fig. 1. Note that in panel (d) the red and grey curves practically overlap.

of (15) preserve the norm S (see appendix of [28] for more details). For this reason the corresponding relative error S_r attains smaller values than for the ABC^2 and SS^2 integrators (Fig. 1c). From Fig. 1d we see that the SIFT^2 integration scheme is the most efficient one with respect to the CPU time needed for obtaining the results of Fig. 1.

For this reason we use the SIFT^2 SI as a reference method, and compare in Fig. 2 its results with the ones obtained by the fourth order SIs: ABC$^4_{[Y]}$, ABC$^4_{[S]}$, SIFT^4 and SS^4. These SIs reproduce correctly the evolution of m_2 (Fig. 2a) and keep $E_r \approx 10^{-5}$ (Fig. 2b). S_r for the SIFT^4 method shows a similar behavior to SIFT^2, while for all other integrators it attains larger, slowly increasing values, which nevertheless remain acceptably small (Fig. 2c). The SIFT^4 method requires more CPU time than SIFT^2 (Fig. 2c), despite the fact it utilizes a larger time step, because it implements the CPU time consuming Fourier transforms more times. Consequently, the development of higher order schemes based on Fourier transforms for the integration of the $\mathcal{B}$ part of Hamiltonian (15) does not lead to very efficient schemes, with respect to CPU time requirements. From the remaining integrators of Fig. 2 the ABC$^4_{[Y]}$ requires the least CPU time (Fig. 2d).

Therefore, we compare in Fig. 3 this integrator with the remaining fourth order schemes that we consider in our study: SIFT$^4_{864}$, SIFT$^4_{1064}$, SS$^4_{864}$ and SS$^4_{1064}$. Again all schemes accurately reproduce the evolution of m_2 (Fig. 3a) and keep the relative energy error practically constant, i.e. $E_r \approx 10^{-5}$ (Fig. 3b). The SIFT$^4_{864}$ and SIFT$^4_{1064}$ methods, which implement Fourier transforms, have again small S_r values, while SS$^4_{864}$ and SS$^4_{1064}$ methods preserve the norm quite accurately as they produce (larger) S_r values, which nevertheless remain practically constant (Fig. 3c). The good behavior of the SS$^4_{864}$ and SS$^4_{1064}$ integrators is probably due to the fact that the corresponding fourth order ABAH864 and ABAH1064 integrators, on which they are based, also eliminate some higher order terms.

From Fig. 3d we see that all methods considered in Fig. 3 require more or less similar CPU times, with the SS$^4_{864}$ scheme showing the best performance. Nevertheless, one should be more careful about the significance of CPU time improvements. From the results of Fig. 3 we see that using the SS$^4_{864}$ with $\tau = 0.25$ we need

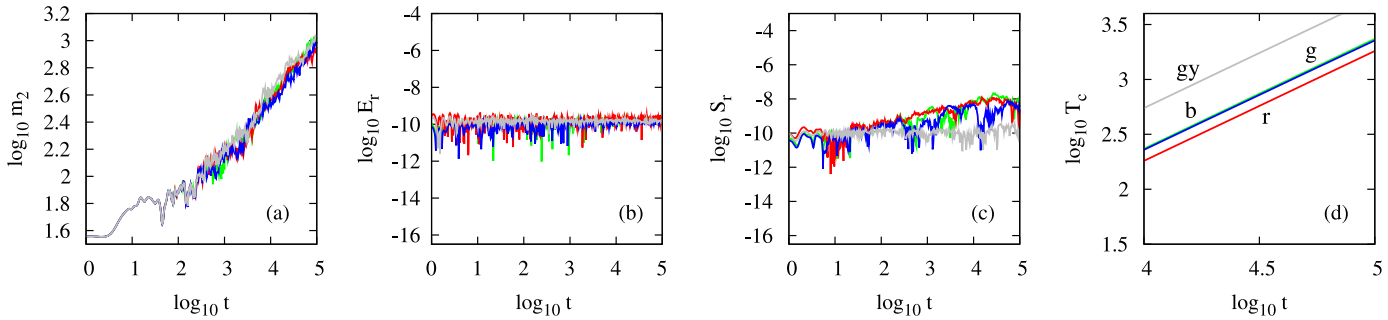

Fig. 4. (Color online.) Results for the integration of H_D (15) by the fourth order SI SS^4_{864} for $\tau = 0.015625$ [(gy) grey], and the sixth order SIs $ABC^6_{[Y]}$ for $\tau = 0.03$, $ABC^6_{[SS]}$ for $\tau = 0.125$ and $ABC^6_{[KL]}$ for $\tau = 0.04$ [(g) green; (r) red; (b) blue]. The panels are as in Fig. 1. Note that in panel (d) the green and blue curves practically overlap.

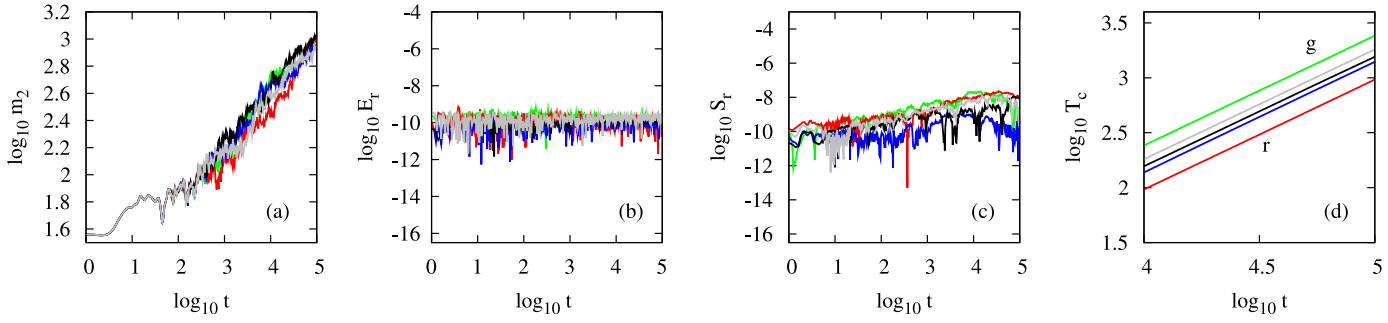

Fig. 5. (Color online.) Results for the integration of H_D (15) by the sixth order SI $ABC^6_{[SS]}$ for $\tau = 0.125$ [grey], the eight order SIs $ABC^8_{[Y]}$ for $\tau = 0.0625$, $ABC^8_{[SS]}$ for $\tau = 0.2$, $ABC^8_{[KL]}$ for $\tau = 0.125$ [(g) green; (r) red; (b) blue], and the tenth order SI $ABC^{10}_{[SS]}$ for $\tau = 0.2$ [(bl) black].

~ 1.2 times less CPU time than the $ABC^4_{[Y]}$ with $\tau = 0.05$, which is the best performing scheme among the ones considered in Figs. 1 and 2. Comparing the SS^4_{864} method with the SS^2 and $SIFT^2$ methods usually used in numerical studies of the DDNLS model [27–31] we see that the gain factor increases even more. In particular, SS^4_{864} scheme requires ~ 1.4 and ~ 2.0 times less CPU time than the $SIFT^2$ with $\tau = 0.05$ and the SS^2 with $\tau = 0.02$ respectively (Fig. 1). Although one might argue that these CPU time gain factors are not too big, we should keep in mind that long time simulations up to $t = 10^7$–10^8 of the DDNLS model with $N \sim 1000$ sites could require (depending on the particular computer used) up to ~ 10 days of computations. Thus a gain factor of 2 is practically significant as it can considerably reduce the computation time.

To keep $E_r \approx 10^{-5}$ most of the studied SIs of order higher than four require large integration steps, which are already outside the stability domain of these algorithms. In order to avoid this situation we lowered the relative energy error to $E_r \approx 10^{-10}$ for the comparative study of these methods. From the results of Fig. 4 we see that, as expected, the sixth order SIs $ABC^6_{[Y]}$, $ABC^6_{[SS]}$ and $ABC^6_{[KL]}$ are more efficient than the SS^4_{864} which showed the best performance among all integration schemes of Figs. 1–3, as they correctly reproduce the evolution of m_2 (Fig. 4a), keep bounded both the energy (Fig. 4b) and the norm (Fig. 4c) relative errors (although a slight increase is observed for S_r) and require less CPU time (Fig. 4d).

Implementing SIs of even higher order we obtain methods with even better performances (namely schemes $ABC^8_{[Y]}$, $ABC^8_{[SS]}$, $ABC^8_{[KL]}$ and $ABC^{10}_{[SS]}$) than $ABC^6_{[SS]}$ (Fig. 5). Nevertheless, only the increase of the SI's order is not sufficient to guarantee improvement of the computational behavior, as the simultaneous growth of steps could augment the CPU time requirements. For instance, this is why $ABC^8_{[Y]}$ and $ABC^{10}_{[SS]}$ require more CPU time than $ABC^6_{[SS]}$ and $ABC^8_{[SS]}$ respectively (Fig. 5d).

Our results indicate that the construction of efficient triple split SIs can allow the integration of the DDNLS for longer times, and numerically tackle questions about the asymptotic behavior of wave packets. We note that the $ABC^8_{[SS]}$ SI required the less CPU time among all tested schemes (Fig. 5d).

5. Conclusions and discussion

In summary, we presented ways to use SIs for Hamiltonian systems that do not split in two integrable parts, as traditional symplectic methods require, but in three. For such systems we considered several high order three part split SIs based on already developed composition methods and emphasized their practical importance. In particular, we showed that such three part split SIs are more efficient numerical schemes than other symplectic and non-symplectic methods in terms of both accuracy and CPU time requirements. These characteristics are of particular importance for the long time integration of multidimensional systems like the DDNLS model, whose asymptotic behavior is currently a very debatable issue.

Many of the studied integration schemes showed a quite satisfactory behavior with respect to both their accuracy and efficiency. For example integrator SS^4_{864} required the least CPU time among all tested schemes of order up to four and kept practically constant also the relative error of the system's second integral of motion i.e. its norm. In addition, all algorithms based on the integration of the $\mathcal{B} = B + C$ part of Hamiltonian (15) via Fourier transforms, i.e. methods $SIFT^2$, $SIFT^4$, $SIFT^4_{864}$ and $SIFT^4_{1064}$ succeeded in keeping the relative error S_r very low (although it increased with integration time). A drawback of these methods is that, due to the applications of Fourier transforms, they require the number of lattice sites to be 2^k, $k \in \mathbb{N}^*$, although this is not always the case in numerical simulations. Also schemes referred as ABC methods, which are based on the fact that the studied Hamiltonian (15) is split in exactly three integrable parts, proved to be quite efficient methods, whose performance generally improve with increasing order.

We hope that our results will draw the interest of the community in the construction of three part split SIs, and will initiate

future research both for the theoretical development of new, improved integrators of this type, as well as for their applications to different dynamical systems. Keeping in mind that such SIs can provide efficient numerical schemes for the long time integration of Hamiltonian systems with many degrees of freedom (like the DDNLS model), it would be interesting to investigate if the possible addition of a corrector term can improve their accuracy, as done for traditional two part split methods (see e.g. [11]).

Acknowledgements

We thank the anonymous referee for many valuable suggestions that helped us to greatly improve our paper. Ch.S. would like to thank S. Anastasiou, G. Benettin and J. Laskar for useful discussions, as well as the Max Planck Institute for the Physics of Complex Systems in Dresden for its hospitality during his visits in 2012 and 2013, when part of this work was carried out. Ch.S. was supported by the Research Committee, Aristotle University of Thessaloniki (Prog. No. 89317) and the University of Cape Town (Start-Up Grant, Fund No. 459221), as well as by the European Union (European Social Fund – ESF) and Greek national funds through the Operational Program "Education and Lifelong Learning" of the National Strategic Reference Framework (NSRF) – Research Funding Program: "THALES. Investing in knowledge society through the European Social Fund". S.E. acknowledges the support of the European Union Seventh Framework Program (FP7/2007-2013) under grant agreement No. 282703. E.G. would like to thank P. Jung for fruitful discussions.

References

[1] E. Hairer, C. Lubich, G. Wanner, Geometric Numerical Integration. Structure-Preserving Algorithms for Ordinary Differential Equations, Springer Series in Computational Mathematics, vol. 31, Springer, New York, 2002.
[2] R.I. McLachan, G.R.W. Quispel, J. Phys. A 39 (2006) 5251.
[3] É. Forest, J. Phys. A 39 (2006) 5321.
[4] H. Yoshida, Phys. Lett. A 150 (1990) 262.
[5] É. Forest, R.D. Ruth, Physica D 43 (1990) 105.
[6] J. Candy, W. Rozmus, J. Comput. Phys. 92 (1991) 230.
[7] R.I. McLachan, P. Atela, Nonlinearity 5 (1992) 541.
[8] H. Yoshida, Celest. Mech. Dyn. Astron. 56 (1993) 27.
[9] R.I. McLachan, BIT Numer. Math. 35 (1995) 258.
[10] S.A. Chin, Phys. Lett. A 226 (1997) 344.
[11] J. Laskar, P. Robutel, Celest. Mech. Dyn. Astron. 80 (2001) 39.
[12] S. Blanes, F. Casas, A. Farrés, J. Laskar, J. Makazaga, A. Murua, Appl. Numer. Math. 68 (2013) 58.
[13] A. Farrés, J. Laskar, S. Blanes, F. Casa, J. Makazaga, A. Murua, Celest. Mech. Dyn. Astron. 116 (2013) 141.
[14] P.J. Channell, F. Neri, Fields Inst. Commun. 10 (1996) 45.
[15] J.E. Chambers, Mon. Not. R. Astron. Soc. 304 (1999) 793.
[16] K. Goździewski, S. Breiter, W. Borczyk, Mon. Not. R. Astron. Soc. 383 (2008) 989.
[17] T. Quinn, R.P. Perrine, D.C. Richardson, R. Barnes, Astron. J. 139 (2010) 803.
[18] J.E. Chambers, in: N. Haghighipour (Ed.), Planets in Binary Star Systems, in: Astrophysics and Space Science Library, vol. 366, 2010, p. 239.
[19] P.-V. Koseleff, Fields Inst. Commun. 10 (1996) 103.
[20] I.P. Omelyan, J. Chem. Phys. 127 (2007) 044102.
[21] W. Kahan, R.-C. Li, Math. Comput. 66 (1997) 1089.
[22] M. Sofroniou, G. Spaletta, Optim. Methods Softw. 20 (2005) 597.
[23] S. Blanes, F. Casas, A. Murua, Bol. Soc. Esp. Mat. Apl. 45 (2008) 89.
[24] M. Suzuki, Phys. Lett. A 146 (1990) 319.
[25] R.I. McLachan, SIAM J. Sci. Comput. 16 (1995) 151.
[26] G. Kopidakis, S. Komineas, S. Flach, S. Aubry, Phys. Rev. Lett. 100 (2008) 084103.
[27] S. Flach, D.O. Krimer, Ch. Skokos, Phys. Rev. Lett. 102 (2009) 024101.
[28] Ch. Skokos, D.O. Krimer, S. Komineas, S. Flach, Phys. Rev. E 79 (2009) 056211.
[29] T.V. Laptyeva, J.D. Bodyfelt, D.O. Krimer, Ch. Skokos, S. Flach, Europhys. Lett. 91 (2010) 30001.
[30] J.D. Bodyfelt, T.V. Laptyeva, Ch. Skokos, D.O. Krimer, S. Flach, Phys. Rev. E 84 (2011) 016205.
[31] J.D. Bodyfelt, T.V. Laptyeva, G. Gligorić, D.O. Krimer, Ch. Skokos, S. Flach, Int. J. Bifurc. Chaos Appl. Sci. Eng. 21 (2011) 2007.
[32] M. Johansson, G. Kopidakis, S. Aubry, Europhys. Lett. 91 (2010) 50001.
[33] S. Aubry, Int. J. Bifurc. Chaos Appl. Sci. Eng. 21 (2011) 2125.
[34] Freely available from http://www.unige.ch/~hairer/software.html.